


In situ Photocrosslinkable Hyaluronic Acid-Based Surgical Glue with Tunable Mechanical Properties and High Adhesive Strength

Ajeesh Chandrasekharan,¹ Keum-Yong Seong,¹ Sang-Gu Yim,¹ Sodam Kim,¹ Sungbaek Seo,¹ Jinhwan Yoon,² Seung Yun Yang ¹

¹Department of Biomaterials Science, Life and Industry Convergence Institute, Pusan National University, Miryang 50463, Republic of Korea

²Department of Chemistry Education, Graduate Department of Chemical Materials, Pusan National University, Busan 46241, Republic of Korea

Correspondence to: S. Y. Yang (E-mail: syang@pusan.ac.kr)

Received 1 October 2018; Accepted 13 November 2018; published online 7 December 2018

DOI: 10.1002/pola.29290

ABSTRACT: Hyaluronic acid (HA), a naturally occurring linear polysaccharide, has been widely used as a key biomaterial in a range of cosmetic and therapeutic applications. Its excellent biocompatibility and bio-functions related to tissue regeneration encourage the development of HA-based hydrogels to expand its applications. This study details an *in situ* forming surgical glue based on photocrosslinkable HA, providing tunable mechanical properties and firm tissue adhesion under wet and dynamic conditions. Depending on the degree of photocrosslinkable methacrylate groups in HA polymer chains, the mechanical properties of hyaluronate methacrylate (HAMA) hydrogels prepared by UV

photocrosslinking was improved. *Ex vivo* adhesion tests revealed that HAMA hydrogels exhibited 3-fold higher shear adhesive strength compared to gelatin methacryloyl hydrogels and achieved firm adherence to the porcine skin tissue for several weeks. The high adhesive strength of HAMA hydrogels, under dry and wet conditions, suggests that it may have great promise as a tissue adhesive. © 2018 Wiley Periodicals, Inc. *J. Polym. Sci., Part A: Polym. Chem.* **2019**, *57*, 522–530

KEYWORDS: adhesives; biomaterials; crosslinking; hyaluronic acid; photocrosslinkable polymer; surgical glue; tissue adhesive

INTRODUCTION Tissue adhesives are emerging as an alternative or adjunct to sutures and staples for wound closure owing to their ease of preparation and application, strong adhesion to the wound site, and effective sealing of body fluids. In addition, they can also be encapsulated with drugs or growth hormones to promote wound healing.^{1–5} Tissue adhesives can be broadly classified into patch and glue-type adhesives. In both these types, the main focus has been on improving the adhesion strength by utilizing novel biomaterials and techniques or by tailoring material properties. For patch-type adhesives, research has primarily focused on mimicking the adhesion strategies used by land and/or aquatic animals such as geckos, marine mussels, and endoparasitic worms to enhance adhesion.^{6–10} Gecko-inspired adhesive patches generally consist of an array of nanofabricated polymer pillars mimicking the feet of a gecko. It was also coated with a synthetic polymer that can mimic the proteins found in mussel holdfasts to increase the adhesion under wet conditions.⁷ In contrast, an endoparasitic worm-inspired microneedle adhesive patch has swellable tips, which when inserted into the tissue can swell and mechanically interlock with the

tissues.⁸ As this design also provides a minimally invasive way to deliver a drug across the stratum corneum of the skin, it has been used as a drug delivering adhesive patch.^{9–11} However, glue-type tissue adhesives have recently gained attention as they can flow into the wound cracks providing strong adhesion between the tissues and the glue, effectively preventing leakage of body fluids. In addition, it can be prepared *in situ*, and the mechanical properties can be tuned to suit the surrounding tissue, which enables it to be used for tissues with different geometry and dimensions.^{2,3,12–14}

Glue-type tissue adhesives are comprised of either synthetic or biologically derived materials or a mixture of both and have been previously developed and used. This type of adhesive is generally comprised of monomers and/or polymers functionalized with reactive groups such as nitrile, thiol, glutaryl-succinimidyl ester, and acrylate.⁴ When these are applied on to a tissue they can form covalent bonds with functional groups present on the tissues, or they can be activated by chemicals (chemical crosslinking) and light (photocrosslinking) to form three-dimensional cross-linked networks.³ For example, a cyanoacrylate-based adhesive

Additional supporting information may be found in the online version of this article.

© 2018 Wiley Periodicals, Inc.

comprised of a synthesized monomer, butyl-2-cyanoacrylate, consists of alkyl, nitrile and acrylate groups; acrylate groups react with basic hydroxyl ions present on tissues to form covalent bonds between the glue and tissue.¹⁵ The cyanoacrylate-based adhesives are an attractive candidate for wound closure because of the ease of preparation, fast curing rate, and strong adhesion to the tissues.^{16,17} However, they still have certain limitations such as poor flexibility, weak adhesion in wet and dynamic conditions, and a toxic degradation product, which limits its application to only topical use.^{18,19} In the case of biologically derived glue-type adhesives, the most widely used in clinical applications are fibrin-based glues. Although it has certain advantages such as fast curing, biocompatibility, and biodegradability, the risk of infection resulting from the biological sources is a major safety concern.²⁰ In addition, fibrin-based glues show weak adhesion on wet surfaces, limiting its use under wet conditions.²¹

Recently, hydrogel-based adhesives are being widely explored due to their advantages such as biocompatibility, biodegradability, tunable mechanical properties, and high water absorbing capacity, which keep the wound site wet and allow natural healing to occur.^{22,23} As hydrogels are a three-dimensional polymeric network, it can also be used as a drug delivering matrix to enhance tissue regeneration processes.³ For example, CoSeal™ is a well-known hydrogel-based adhesive that is used for sealing suture lines and vascular grafts.²⁴ It consists of two four-armed branched polyethylene glycol (PEG) polymers, one end capped with thiol groups and the other with glutaryl-succinimidyl ester. When required, solutions of these two PEG polymers are mixed and sprayed at the wound site; the thiol group reacts with glutaryl-succinimidyl ester groups to form covalently crosslinked hydrogel networks.²⁵ While PEG is a non-toxic, non-immunogenic, and biocompatible polymer, hence having been used both *in vitro* and *in vivo*, it requires more caution while applying in closed spaces as it has a high swelling ratio of up to 400%.²⁶ In addition, because of its inert characteristics, it does not promote wound healing processes.²⁷

Photocrosslinking technique allows for *in situ* crosslinking of the precursor solution, and gives better spatial and temporal control over the crosslinking density than chemical crosslinking techniques.²⁸ The photocrosslinking methods using ultraviolet (UV) or visible light have been used to prepare hydrogels with wide range of mechanical properties and degradability.^{2,15} For example, visible light has been used to prepare hydrogels with comparative mechanical properties with that of hydrogels prepared by UV crosslinking.²⁹ However, the common initiators used in this method such as eosin Y and ruthenium complex showed less biocompatibility.^{1,30} More recently, using azide functionalized moiety, photocrosslinking was reported without the use of photoinitiator.³¹ Nevertheless, UV photocrosslinking technique has been widely used in various biomedical applications including tissue adhesives owing to its suitability for application to weakened tissues with fast curing kinetics.³² Recently, a UV photocrosslinkable gelatin methacryloyl (GelMA) based

sealant was shown to have adhesive strength higher than some of the commercially available adhesives and sealants.¹³ However, the GelMA hydrogel was reported to have shown rapid degradation *in vivo*. The main limitations of gelatin-based biomaterials are weak mechanical properties and rapid degradation.^{33–36} Taking into consideration the limitations exhibited by the currently available tissue adhesives on the market, there is a need for a tissue adhesive that has strong adhesion to the tissue under wet and dynamic conditions for a long period of time to allow for wound healing. Ideally, it should last for 3 weeks before it starts degrading and should be completely degraded in 3 months.⁴ In addition, the biomaterial used must have excellent biocompatibility to prevent an inflammatory response and tunable mechanical properties to suit that of the surrounding tissue to avoid a foreign body reaction, as these might hinder the wound healing process.^{37,38}

Hyaluronic acid (HA) is a linear polysaccharide found in the extracellular matrix of soft tissues and has excellent biocompatibility. It has been shown to play a crucial role in cellular processes such as proliferation, angiogenesis, migration, and improving scarless wound healing processes. In addition, the high water absorbing capacity of HA facilitates the diffusion of nutritional supplies to the wound site, further aiding in wound healing processes.^{39–42} These properties make HA an ideal candidate for promoting wound healing and tissue regeneration. HA can be chemically functionalized with photocrosslinkable methacrylate or acrylate groups to obtain photocrosslinked hydrogels.⁴³ However, acrylate groups have not been well studied in tissue engineering applications, especially in wound healing. In addition, hydrogels produced from hyaluronate methacrylate (HAMA) have been shown to facilitate cell infiltration and angiogenesis, a prerequisite for wound healing.⁴⁴ HAMA hydrogels undergoes complete enzymatic degradation in the presence of hyaluronidase but has been shown to have slow degradation behavior depending on their crosslinking density.^{45,46} These properties make HAMA a good candidate as a tissue adhesive. Previously, HAMA has been studied as a tissue adhesive.¹⁴ This hydrogel adhesive showed good adherence to tissue but its low degree of methacrylation (DM) might limit its use to manipulate material properties of the photocrosslinked hydrogels.

In this work, we engineered an *in situ* photocrosslinkable tissue adhesive based on HA, a well-known biopolymer. HAMA with a low and high DM was synthesized and confirmed by ¹H NMR. First, the mechanical properties of HAMA hydrogels prepared from different concentration (5%, 10%, and 20% [w/v]) of precursor solutions at a low and high DM were investigated using a tensile test to evaluate its tunability. Then, we evaluated the cohesive and adhesive properties of the HAMA hydrogels produced from a high DM. Its mechanical and adhesive properties were investigated by several standard tests including the tensile test, *in vitro* wound closure test, and lap shear test; the results were compared to that of the GelMA hydrogels produced from a high DM. Finally, to

determine the adhesion capability of the HAMA hydrogels under wet and dynamic conditions, the HAMA hydrogels formed on porcine skin were placed under wet and dynamic conditions and their adherence to the porcine skin were measured for several weeks.

EXPERIMENTAL

Synthesis and Characterization of the Photocrosslinkable HAMA

About 1.0 g HA (M_w : 90,000 kDa; SNvia, Korea) was dissolved in 12 mL distilled water and the pH was adjusted to 8.0 using 1 N sodium hydroxide. The HA solution was cooled down to 5 °C and then 1 or 4 equivalents of methacrylic anhydride (MA) with respect to disaccharide unit of HA was added dropwise over a period of 1 h. The pH was simultaneously maintained between 8.0 and 10.0 by adding 1 N sodium hydroxide. The temperature and pH were maintained for another 23 h, after which the macromer solution was dialyzed (Cellu Sep, nominal molecular weight cutoff 3500 Da) against distilled water for 3 days, frozen at -55 °C, lyophilized, and stored at -20 °C until use. ^1H NMR spectrum was obtained using a Bruker 600-NMR spectrometer. This was used to confirm the incorporation of methacrylate groups into HA and to calculate the DM ($n = 3$).

Preparation of HAMA/GelMA Hydrogels

Precursor solutions were prepared by first dissolving 1.0% (w/v) 1-[4-(2-Hydroxyethoxy)-phenyl]-2-hydroxy-2-methyl-1-propane-1-one (Sigma-Aldrich) of photoinitiator in distilled water at 60 °C, followed by dissolving HAMA/GelMA solid to get 5% (w/v), 10% (w/v), and 20% (w/v) precursor solutions. Hydrogels were prepared by photocrosslinking with UV light (320–500 nm, ~30 mW cm⁻², OmniCure S1500) for an exposure time of 20 to 60 s depending on the dimensions of the HAMA/GelMA hydrogels.

Characterization of Mechanical Properties

Briefly, polymer precursor solutions at different concentrations of 5% (w/v), 10% (w/v), and 20% (w/v) were photocrosslinked to produce the following geometries: tensile testing (20 mm in length, 5 mm in width, and 1.5 mm in thickness). The hydrogels were directly analyzed on a mechanical tester (AND 210, Korea). The strain rate was set to 1 mm min⁻¹ for tensile testing. The ultimate tensile strengths of the samples were determined at the point of failure (fracture under tensile) of the hydrogels. The tensile strength was determined at the maximum point of stress in the stress-strain curves. The Young's modulus was calculated by obtaining the initial 5% of the slope in the strain-stress curves. The elasticity was determined at the maximum point of strain in the stress-strain curves.

Scanning Electron Microscopy

Photocrosslinked HAMA hydrogel samples were produced from 5% (w/v), 10% (w/v), and 20% (w/v) of HAMA in precursor solutions and they were lyophilized and mounted onto an aluminum holder. A 10-nm thick gold layer was spin-

coated on the sample prior to imaging. Secondary electron imaging was performed at 10 kV using a Hitachi FE-SEM s-4700. The effects of HAMA concentrations on the pore size of HAMA hydrogels were investigated.

In Vitro Lap Shear Test

Shear strength of HAMA/GelMA was examined according to the standard testing method for strength properties of tissue adhesives under lap-shear by tension loading, ASTM F2255-05, as previously described.¹ Gelatin 20% (w/v) was dissolved in PBS at 80 °C, which was then coated (10 × 15 mm) on top of glass slides (10 × 50 mm). Gelatin on glass slides were then dried at 60 °C for 2 h, before cooling down to room temperature. Next, 40 μL of HAMA/GelMA precursor solution was dropped on top of the gelatin coating of a glass slide, after which another gelatin-coated glass slide was placed over the adhesive. This was followed by irradiation with UV light. The two glass slides were placed onto a mechanical tester (AND 210, Korea) for shear testing by tensile loading with a strain rate of 1 mm min⁻¹. The shear strength was determined at the point of maximum stress. Six replicates were conducted for each concentration of HAMA/GelMA solutions.

In Vitro Wound Closure Test

The adhesion strength of the adhesive was determined by using the standard test method for wound closure strength of tissue adhesives and sealants, ASTM F2458-05, with some modification as described in the literature.¹ In brief, fresh porcine skin purchased from a local slaughterhouse was cut into rectangular sections (5 × 15 mm). While unused, porcine skin was kept moist in gauze soaked in PBS. Before use, porcine skin was blotted dry to remove excess liquid, and each end of the skin strip was fixed onto two glass slides (10 × 50 mm) with glue, leaving a 6 mm section of skin between the slides. The porcine skin strip was then cut apart using a razor blade, and petroleum jelly was applied with a syringe to the ends of the desired adhesive application area in order to confine the precursor solution before crosslinking. Afterward, 40 μL of the HAMA/GelMA precursor solution was dropped on the porcine skin and was irradiated with UV light. The two glass slides were placed onto a mechanical tester (AND 210, Korea) for adhesive strength testing by tensile loading with a strain rate of 1 mm min⁻¹. The adhesive strength was determined at the maximum point of detachment. Five repeats were conducted for each concentration of HAMA/GelMA solutions.

In Vitro Adhesion Test Under Wet and Dynamic Conditions

Fresh porcine skin was cut into a rectangular shape (10 × 20 mm) and soaked in the PBS for a minimum of 2 h before it was used. The porcine skin was glued to a glass microscope slide (10 × 50 mm), and a wound (6 × 1 mm) was created using a biopsy punch. While unused, porcine skin was kept moist in gauze soaked in PBS. Before use, porcine skin was blotted dry to remove excess liquid. A PDMS mold (8 × 3 mm) was placed on top of the cut area and,

HAMA precursor solution (126 μ L) was poured into the mold. This was followed by irradiation with UV light, and the PDMS was gently removed. The slide fixed with porcine skin was immersed in a 250-mL beaker containing 150 mL PBS (pH 7.4) at 37 $^{\circ}$ C. To mimic a dynamic environment, a magnetic stirrer bar was rotated at a speed of 1000 rpm to generate flow. The number of hydrogels adhered to the porcine skin was recorded every day, and the PBS in the beaker was replaced with fresh PBS. Three repeats were conducted for each concentration of HAMA solutions.

RESULTS AND DISCUSSION

Synthesis and Characterization of HAMA Hydrogels

Photocrosslinkable methacrylate groups are generally incorporated into an HA polymer backbone by reacting it with MA under aqueous basic conditions.^{44,47} The primary hydroxyl group in HA is considered the most reactive site for transesterification [Fig. 1(a)]. HA has four hydroxyl groups per disaccharide unit, all of the four hydroxyl groups could be incorporated with methacrylate groups. Previously, by varying the molecular weight of HA, molar ratio of MA to HA, and reaction time, HAMAs with different DM have been synthesized.^{48,49} There are also other parameters that determine the DM such as pH and temperature of the reaction mixture.⁵⁰ MA undergoes hydrolysis in an aqueous medium, especially above pH 10.0, catalyzed by hydroxide ion to form methacrylic acid, which does not react with HA.⁵¹ At low temperatures, hydrolysis of MA to methacrylic acid is considered to be slower. However, at this temperature MA exists in a separate phase.⁵⁰

HA is known to play an important role in wound healing processes. HAs with a MW of 100–300 kDa have been shown to improve wound healing by promoting angiogenesis.⁵² Considering its biological activities and better solution processability, 90 kDa HA was chosen. In order to synthesize HAMA with different DM, 1 or 4 equivalents of MA with respect to the disaccharide unit was reacted with HA. Furthermore, to minimize the excess hydrolysis of MA and to reduce the phase separation during the reaction, it was added dropwise over a period of 1 h with vigorous stirring. Simultaneously, the pH was maintained between 8.0 and 10.0 at 5 $^{\circ}$ C for 24 h. Details regarding the synthesis of GelMA are provided in the Supporting Information.

The proton NMR experiment was used to determine the incorporation of methacrylate groups into HA and the DM. The NMR spectrum revealed new peaks around δ 5.6 and 6.0 ppm corresponding to acrylate protons, suggesting incorporation of methacrylate groups into HA [Fig. 1(b)]. The DM was calculated from the relative integration of the methacrylate protons (5.6 and 6.0 ppm) to the methyl protons in HA (1.9 ppm), and this gave a value of $46 \pm 4\%$ and $181 \pm 36\%$, per disaccharide unit for 1- and 4-equivalent of MA, respectively. The peaks corresponding to acrylate protons (7,8) and methyl protons (10) used for DM calculation is presented in Supporting Information Figure S1. The molecular weights of HA and its derivatives were estimated with a gel permeation chromatography system (Supporting Information Fig. S2). They showed similar polymer molecular weight distribution, indicating no premature crosslinking or significant chain cleavage during the reaction. Above 100% methacrylation suggests that more than one hydroxyl group was substituted when 4-equivalent of MA was used. Previously, incorporation of methacrylate groups into HA has been reported with varying DM (7–160%).^{44,46,53} However, there are only a few reports with a high (>100%) DM and, in those reports a high molar ratio (10- to 20-equivalent) of MA was used.^{43,44} For example, Seidlits *et al.* have used 10- and 20-fold molar excess of MA to HA to achieve 87 ± 22 and $160 \pm 32\%$ DM, respectively.⁴⁴ Our results suggest that by carefully minimizing excess hydrolysis of MA by the slow addition of MA over a period of 1 h with vigorous stirring and maintaining the pH between 8.0 and 10.0 for 24 h at 5 $^{\circ}$ C, a high DM (>100%) can be obtained with a 4 equivalents of MA. The GelMA NMR spectrum revealed new peaks at 5.6 and 5.8 ppm corresponding to methacrylamide protons (Supporting Information Fig. S3). In addition, methacryl protons corresponding to methacrylation of hydroxyl groups were seen at 5.85 ppm. Absence of a peak at 3.1 ppm, which corresponds to a lysine methylene peak, suggested quantitative conversion of lysine amino groups. Considering this and substitution at the hydroxyl position of gelatin, this could literally be considered as the maximum possible substitution, suggesting a high DM (>100%).

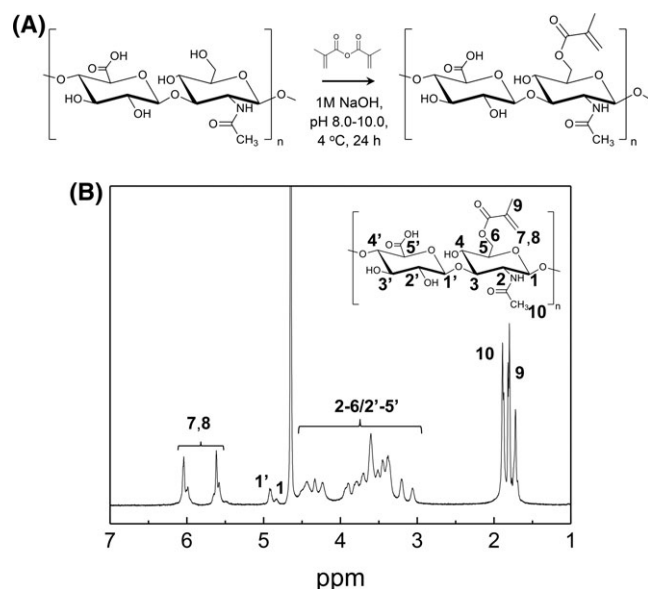


FIGURE 1 (A) Reaction scheme to prepare HAMA and (B) representative ^1H NMR spectrum of HAMA. Peaks correspond to methacrylate protons (7, 8) and methyl protons of HA (10).

gelation and to minimize the cytotoxicity, a light intensity of $\sim 30 \text{ mW cm}^{-2}$ (320–500 nm) and exposure time of 20 to 60 s were used. To tune the mechanical properties of HAMA hydrogels, different degrees of methacrylation (low and high) and concentration (5%, 10%, and 20% [w/v]) were investigated (Fig. 2). Then, to compare the mechanical properties of the HAMA and GelMA hydrogels, the mechanical properties of the GelMA hydrogels produced from varying the concentration (5%, 10%, and 20% [w/v]) at a high DM were tested under the same experimental conditions. The results were compared to those obtained with the corresponding HAMA hydrogels produced from a high DM. The stress–strain curves of 5%, 10%, and 20% (w/v) HAMA hydrogels produced from a low and high DM are shown in Figure 2(a). GelMA hydrogels prepared from 5%, 10%, and 20% (w/v) precursor solutions were investigated as a control [(Supporting Information Fig. S4(a)]. The tensile tests on HAMA hydrogels showed a consistent increase in tensile strength from 3.31 ± 0.61 to 21.22 ± 6.48 kPa and 8.83 ± 2.99 to 44.24 ± 7.09 kPa for low and high DM, respectively, as the concentration of HAMA in the precursor solution was increased from 5% to 20% (w/v) [Fig. 2(b)]. The HAMA hydrogels also exhibited an increasing trend in Young's modulus as the DM and concentrations were increased in the precursor solution [Fig. 2(c)]. The Young's modulus of 10% and 20% HAMA hydrogels at a low DM and that of the 5% and 10% HAMA hydrogels at high DM were 92.11 ± 55.89 , 118.08 ± 51.19 , 183.37 ± 68.37 kPa, and 282.26 ± 45.87 kPa, respectively. These values were within the range of the reported Young's modulus for the dermis layer (~ 88 – 300 kPa).⁵⁴ The elongation for HAMA

hydrogels was between 6 and 17% as the DM and the concentrations were varied [Fig. 2(d)].

Next, the internal structure of HAMA hydrogels were measured using a scanning electron microscope (SEM) to examine crosslinking densities. Although lyophilization might create artificial pores, all the hydrogels were prepared under the same experimental conditions and lyophilized at the same freezing temperature and duration to avoid any differences. The SEM images revealed a decrease in pore sizes with an increase in the DM and concentration [Fig. 2(e)]. This indicates increased crosslinked density for hydrogels prepared from a high DM and higher concentrations of HAMA in precursor solutions.

Although GelMA hydrogels also exhibited an increase in tensile strength and Young's modulus with increases in GelMA concentration [Supporting Information Fig. S4(b,c)], it was relatively lower than that of the corresponding HAMA hydrogels produced from a high DM. For example, 20% GelMA hydrogels exhibited tensile strength and Young's modulus of 24.99 ± 4.32 and 91.07 ± 19.09 kPa, respectively. This was 1.7- and 5.7-fold lower than that of the 20% HAMA hydrogels (44.24 ± 7.09 , 522.24 ± 86.78 kPa). However, GelMA hydrogels exhibited better elongation. The elongation for GelMA hydrogels were between 32 and 38% [Supporting Information Fig. S4(d)] as the concentrations were varied from 5% (w/v) to 20% (w/v). A similar elongation range between 30 and 40% was previously reported for 10% to 25% GelMA hydrogels.¹⁵ This suggested HAMA hydrogels exhibited relatively

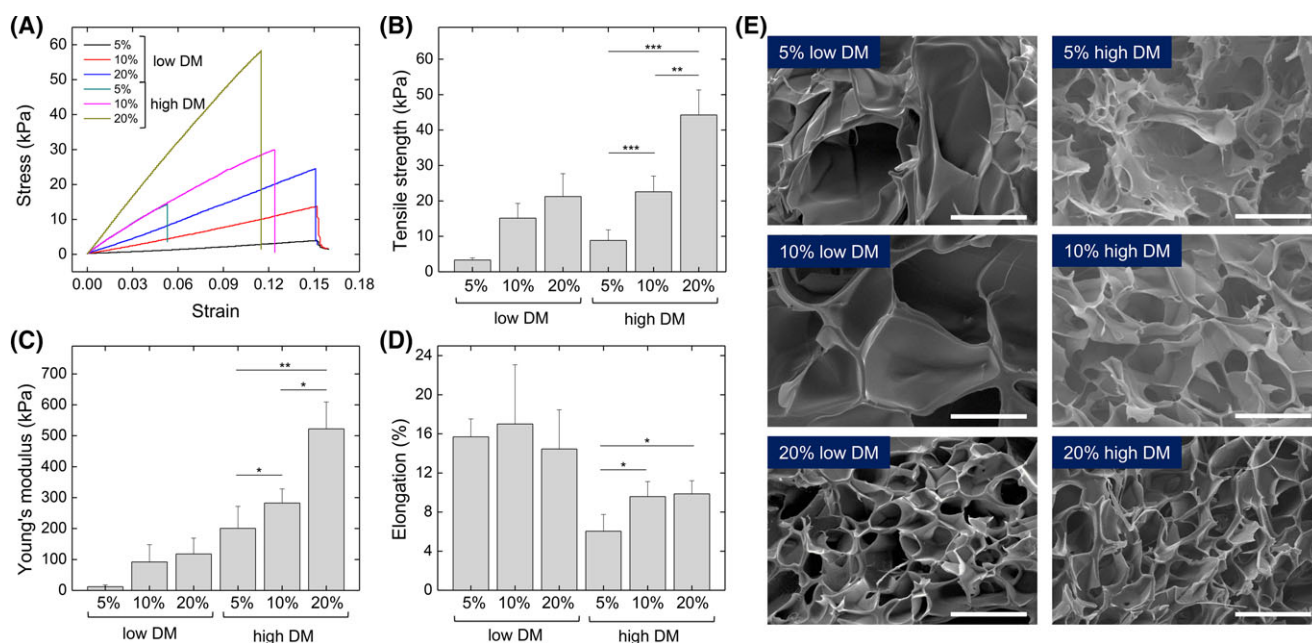


FIGURE 2 Tensile tests on the HAMA hydrogels produced from different concentrations (5%, 10%, and 20% [w/v]) of HAMA solution ($n = 5$) at low and high DM. (A) Representative tensile stress–strain curves, (B) tensile strength, (C) Young's modulus, and (D) elongation. (E) Representative SEM images of the HAMA hydrogels fabricated from 5%, 10%, and 20% (w/v) HAMA solutions at low and high DM (scale bars; 50 μm). Asterisks mark statistical significance levels of $p < 0.05$ (*), $p < 0.01$ (**), and $p < 0.001$ (***). [Color figure can be viewed at wileyonlinelibrary.com]

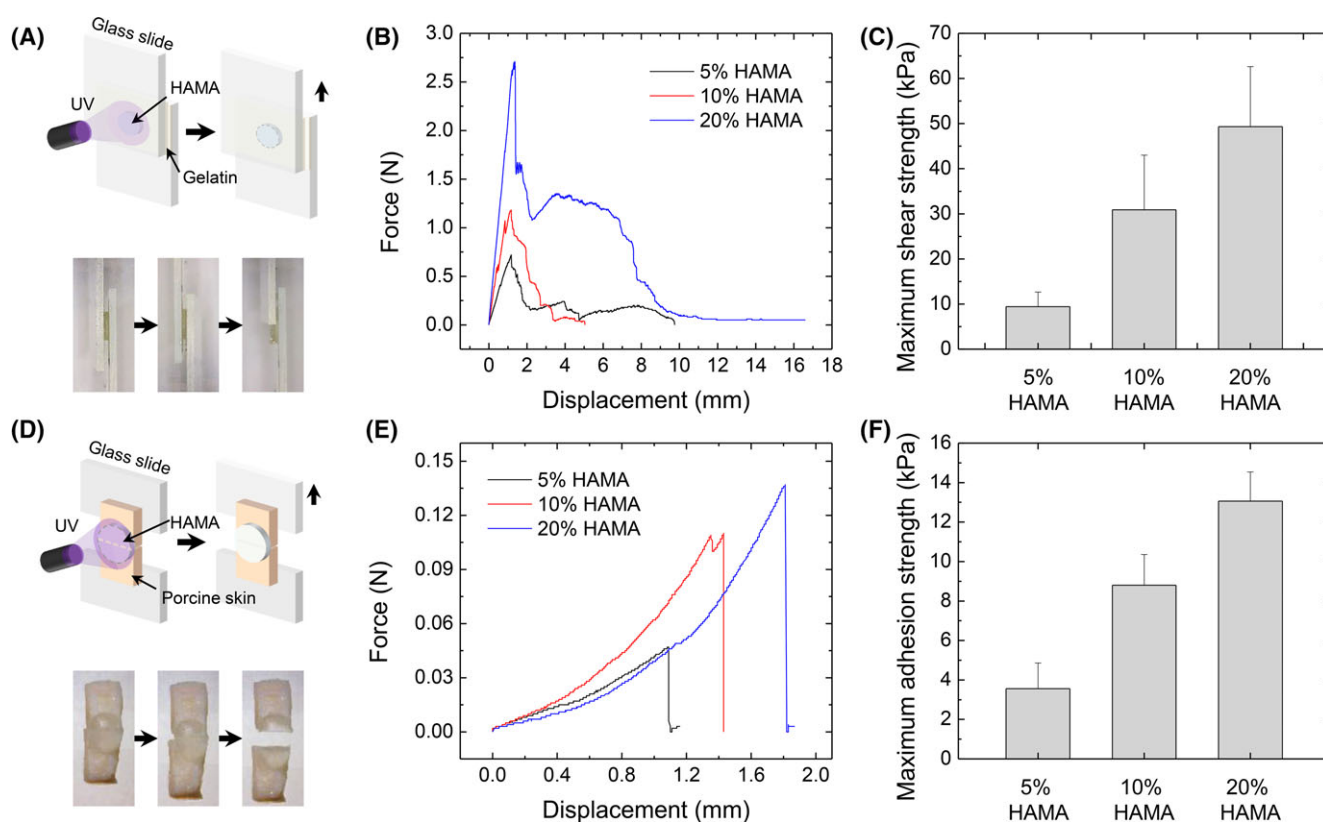


FIGURE 3 (A–C) Lap shear tests to determine the shear strength of HAMA hydrogels produced from 5% (w/v), 10% (w/v), and 20% (w/v) of HAMA in precursor solution at high DM. (A) Schematic illustration and photographs showing the lap shear tests, (B) representative force-displacement curve obtained from lap shear tests, and (C) average maximum shear strength of HAMA hydrogels produced from different concentrations of precursor solution. Error bars represent standard deviation from the mean ($n = 6$). (D–F) Adhesion tests with porcine skin to characterize wound closure performance of the HAMA hydrogels prepared from different concentrations at high DM. (D) Schematic illustration and photographs showing the adhesion tests, (E) representative force-displacement curve obtained from adhesion tests, and (F) maximum adhesive strength of HAMA hydrogels produced from different concentrations of precursor solution. Error bars represent standard deviation from the mean ($n = 6$). [Color figure can be viewed at wileyonlinelibrary.com]

higher stiffness. Nevertheless, comparing the overall mechanical properties of the HAMA and GelMA hydrogels produced from a high DM, the engineered HAMA hydrogels have better cohesive properties.

Hydrogel mechanics is one of the important drivers that determine the efficacy of a tissue adhesive. While a softer hydrogel can easily deform in a mechanically dynamic environment such as the human body, a stiffer hydrogel can cause a severe foreign body response, inhibiting the wound healing process.³⁸ However, it is also generally accepted that cell proliferation and differentiation increases with the stiffness of the matrix. Cells on the stiffer substrate were seen to have stiffer, more organized cytoskeletons and stable focal adhesions than on the softer substrate.⁵⁵ In addition, the enzymatic degradation of hydrogels has been shown to decrease with an increase in stiffness.³³ Considering these results, it could be suggested that the HAMA hydrogels, which exhibited better cohesive properties, might be able to withstand deformation much better, support cell differentiation and proliferation at

the wound site, as well as allow natural wound healing to occur while degrading slowly. Furthermore, the tensile test results show that the mechanical properties of the HAMA hydrogels can be fine-tuned by varying the DM and concentration in the precursor solution, which is ideal for tailoring the mechanical properties to suit that of the surrounding tissues.

Adhesion Properties of HAMA Hydrogels

To evaluate the adhesive characteristics of the engineered HAMA, standard lap shear and wound closure tests were first performed on the 5%, 10%, and 20% (w/v) HAMA hydrogels at a high DM, and the results were compared with that of the corresponding 5%, 10%, and 20% (w/v) GelMA hydrogels. Furthermore, to determine the usability of the HAMA under *in vivo* conditions, HAMA hydrogels were photocrosslinked to the porcine skin and placed under wet and dynamic conditions. Their survival on the porcine skin was then recorded for several weeks.

Representative force-displacement curves for 5%, 10%, and 20% HAMA hydrogels are shown in Figure 3(b), and for the

5%, 10%, and 20% GelMA hydrogels [Supporting Information Fig. S5(a)]. HAMA hydrogels showed a steady increase in shear strength as the concentration was increased from 5% to 20% [Fig. 3(c)]. The shear strength of 5%, 10%, and 20% hydrogels were 9.14 ± 3.55 , 30.95 ± 12.18 , and 49.30 ± 13.31 kPa, respectively. In comparison to the GelMA hydrogels [Supporting Information Fig. S5(b)], the shear strength of HAMA hydrogels was a minimum of 2-fold higher. In addition, the maximum for the 20% HAMA was 3.2-fold higher than that reported for a fibrin-based adhesive (15.38 ± 2.82 kPa).⁵⁶

Next, the adhesive strength under tensile stress was determined by a standard wound closure test on the native skin (porcine skin). Representative force-displacement curves for 5%, 10%, and 20% HAMA hydrogels are shown in Figure 3 (e) and results for the 5%, 10%, and 20% GelMA hydrogels [Supporting Information Fig. S5(c)]. Hydrogels prepared from 20% (w/v) HAMA concentration in precursor solutions exhibited the highest adhesive strength [Fig. 3(f)]. The adhesive strength of 5%, 10%, and 20% HAMA hydrogels were 3.56 ± 1.295 , 8.80 ± 1.55 , and 13.06 ± 1.47 kPa, respectively. These values were significantly higher than those associated with the corresponding GelMA hydrogels [Supporting Information Fig. S5(d)]. For example, the adhesive strength of 10% and 20% HAMA hydrogels were ~ 5 and 3-fold higher than that of 10% and 20% GelMA hydrogels, respectively. Furthermore, the adhesive strength of the 20% HAMA hydrogels was more than ~ 3.2 -fold higher than that of the reported value for fibrin glue (4.0 kPa), which is one of the most widely used biologically derived adhesives in clinical applications.⁵⁷

The reasons for the photocrosslinkable adhesives having good adhesion to the native skin have been generally attributed to hydrogel-tissue interlocking and covalent bond formation

between the hydrogel and tissue arising from the free radicals generated during photocrosslinking.^{58,59} In addition, for adhesives consisting of hydrophilic polymers, it can also be due to the hydrogen bonding between the free hydroxyl groups in the polymers and the tissue surface.⁶⁰ Thus, these factors might have contributed to the adhesion of both HAMA and GelMA hydrogels. It was observed during a wound closure test that both HAMA and GelMA hydrogels broke at the wound site but did not detach from the porcine skin, suggesting higher adhesive strength than fracture strength. However, HAMA hydrogels broke at a higher force than GelMA hydrogels showing higher fracture strength. This might be due to higher crosslinking density within the HAMA hydrogels. A simple comparison of molar concentration of methacrylate groups in both the HAMA and GelMA at the same concentration shows that the HAMA precursor solution would contain ~ 107 -fold higher concentration of methacrylate groups. This is expected to lead to higher crosslinking density within the HAMA hydrogels resulting in better fracture strength. The molar concentration of HAMA was calculated by taking into consideration the molecular weight of the HA disaccharide unit with methacrylate groups (448 g mol^{-1}) and DM (181%), and it was found to be 4.0 mmol of methacrylate groups per gram of HAMA. Whereas for GelMA, based on a literature method, the molar concentration of methacryloyl (methacrylamide and methacrylate) groups was calculated and found to be $0.0375 \text{ mmol g}^{-1}$ of GelMA.⁶¹ Detailed calculations are provided in the Supporting Information for GelMA. Although the synthesized GelMA has a high DM, it is worth considering that only amino groups in the amino acid lysine and a small percentage of hydroxyl groups in gelatin are generally involved in the reaction with MA. However, the other amino groups present such as the arginine-glycine-aspartic acid and matrix metalloproteinase are not significantly involved.⁶² This limits the options to further incorporate methacrylate groups into gelatin, which

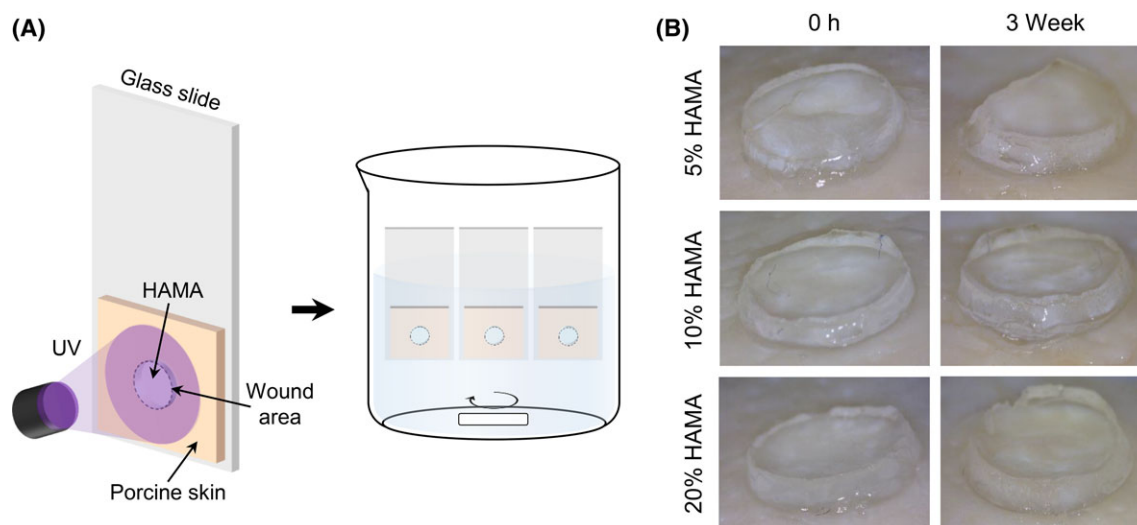


FIGURE 4 Adhesion tests of HAMA hydrogels adhered on porcine skin under wet and dynamic conditions. (A) Schematic of experimental set up for adhesion tests, (B) photographic images of HAMA hydrogels adhered to the porcine skin at 0 h and after 3 weeks. [Color figure can be viewed at wileyonlinelibrary.com]

might account for the GelMA hydrogels exhibiting weaker mechanical properties and faster degradation.

Adhesion Capability of HAMA Hydrogels under Wet and Dynamic Conditions

Next, we conducted *ex vivo* tests to determine the adhesion capability of HAMA hydrogels under wet and dynamic conditions similar to that of the physiological conditions (salt and temperature). In order for a tissue adhesive to be used *in vivo*, it must be able to remain adhered to the target tissue under wet and dynamic conditions. To determine this, precursor solutions consisting of 5%, 10%, and 20% (w/v) of HAMA were dropped on to the wet porcine skin and photocrosslinked by exposure to UV light. The porcine skin with HAMA hydrogels was then placed under a PBS solution at 37 °C and, the solution was stirred at 1000 rpm [Fig. 4(a)]. The 10% and 20% HAMA hydrogels exhibited a firm adhesion to the porcine skin under water for 3 weeks while the 5% HAMA hydrogel showed a partial break at the initial time (2 day after attachment) [Fig. 4(b)]. However, it was observed that a small part of the 5% HAMA hydrogel broke after 2 days, but most parts of the hydrogel remained intact until 3 weeks. These results suggest strong adhesion to the porcine skin as well as the stability of 10% (w/v) and 20% (w/v) HAMA hydrogels under wet and dynamic conditions. Swelling of hydrogels in wet environments could lead to a decrease in mechanical strength and subsequently breakage of the hydrogel.⁶³ Because of the limited water uptake in the highly crosslinked hydrogels,⁶⁴ HAMA hydrogels, especially prepared from high polymer concentration, would undergo less swelling and thus are expected to have good mechanical stability at the wound site. Although HAMA is enzymatically degraded by hyaluronidase, hydrogels with higher crosslinked density degrade at a much lower rate compared to weakly crosslinked hydrogels.⁴⁷ As the long-term residence in wet and dynamic environments may influence the material properties of hydrogels, time-dependent changes in the mechanical and physical properties of the HAMA hydrogels can be considered as a future work. Thus, hydrogels prepared from higher concentrations of HAMA solutions are expected to last longer in physiological environments, and this could be utilized for encapsulation and controlled release of a bioactive molecule for chronic wound healing. Previously, photocrosslinked HAMA has been investigated as a drug delivery system with promising success.⁶⁵ However, safety and toxicity studies have to be conducted to translate this work into clinical application.

CONCLUSIONS

In this work, we have developed an *in situ* photocrosslinkable tissue adhesive based on HA. A systematic investigation was carried out to assess the suitability of the engineered HAMA as a tissue adhesive. The tensile tests revealed that the mechanical properties of HAMA hydrogels can be tailored by varying the DM and concentrations in the precursor solution. The HAMA hydrogels exhibited better cohesive and adhesive properties than that of the corresponding GelMA hydrogels. Under wet and dynamic conditions, the HAMA hydrogels

prepared from higher concentrations of HAMA solution exhibited strong adhesion to the porcine skin for several weeks. Although cytotoxicity and biocompatibility need to be investigated to transfer this work into clinical applications, the tunable mechanical properties as well as strong adhesion to porcine skin under both dry and wet conditions makes HAMA an ideal candidate for tissue adhesive applications.

ACKNOWLEDGMENT

This research was supported by the National Research Foundation of Korea (NRF) funded by the Ministry of Science and ICT (NRF-2018R1A4A1025623).

REFERENCES AND NOTES

- 1 N. Annabi, Y.-N. Zhang, A. Assmann, E. S. Sani, G. Cheng, A. D. Lassaletta, A. Vegh, B. Dehghani, G. U. Ruiz-Esparza, X. Wang, S. Gangadharan, A. S. Weiss, A. Khademhosseini, *Sci. Transl. Med.* **2017**, *9*.
- 2 N. Annabi, D. Rana, E. S. Sani, R. Portillo-Lara, J. L. Gifford, M. M. Fares, S. M. Mithieux, A. S. Weiss, *Biomaterials* **2017**, *139*, 229.
- 3 C. Ghobril, M. Grinstaff, *Chem. Soc. Rev.* **2015**, *44*, 1820.
- 4 P. J. Bouten, M. Zonjee, J. Bender, S. T. Yauw, H. van Goor, J. C. van Hest, R. Hoogenboom, *Prog. Polym. Sci.* **2014**, *39*, 1375.
- 5 P. K. Forooshani, B. P. Lee, *J. Polym. Sci. A: Polym. Chem.* **2017**, *55*, 9.
- 6 K. H. Park, K.-Y. Seong, S. Y. Yang, S. Seo, *Biomater. Res.* **2017**, *21*, 16.
- 7 H. Lee, B. P. Lee, P. B. Messersmith, *Nature* **2007**, *448*, 338.
- 8 S. Y. Yang, E. D. O’Cearbhaill, G. C. Sisk, K. M. Park, W. K. Cho, M. Villiger, B. E. Bouma, B. Pomahac, J. M. Karp, *Nat. Commun.* **2013**, *4*, 1702.
- 9 A. Mahdavi, L. Ferreira, C. Sundback, J. W. Nichol, E. P. Chan, D. J. Carter, C. J. Bettinger, S. Patanavanich, L. Chignozha, E. Ben-Joseph, *Proc. Natl. Acad. Sci. U. S. A.* **2008**, *105*, 2307.
- 10 M. Kim, B. A. Ondrusek, C. Lee, W. G. Douglas, H. Chung, *J. Polym. Sci. A: Polym. Chem.* **2018**, *56*, 1564.
- 11 K.-Y. Seong, M.-S. Seo, D. Y. Hwang, E. D. O’Cearbhaill, S. Sreenan, J. M. Karp, S. Y. Yang, *J. Control. Release* **2017**, *265*, 48.
- 12 F. Scognamiglio, A. Travan, I. Rustighi, P. Tarchi, S. Palmisano, E. Marsich, M. Borgogna, I. Donati, N. de Manzini, S. Paoletti, *J. Biomed. Mater. Res. B: Appl. Biomater.* **2016**, *104*, 626.
- 13 A. Assmann, A. Vegh, M. Ghasemi-Rad, S. Bagherifard, G. Cheng, E. S. Sani, G. U. Ruiz-Esparza, I. Noshadi, A. D. Lassaletta, S. Gangadharan, *Biomaterials* **2017**, *140*, 115.
- 14 J. Shin, J. S. Lee, C. Lee, H. J. Park, K. Yang, Y. Jin, J. H. Ryu, K. S. Hong, S. H. Moon, H. M. Chung, *Adv. Funct. Mater.* **2015**, *25*, 3814.
- 15 J. V. Quinn, *Tissue Adhesives in Clinical Medicine*; PMPH-USA, **2005**; Vol. 2, Chapter 3, pp 32.
- 16 T. Padeganeh, R. Foroghi, A. Bijani, A. Alikhani, *J. Craniomaxillofacial Res.* **2015**, *1*, 45.
- 17 D. W. Bartenstein, D. L. Cummins, G. S. Rogers, *Dermatol. Surg.* **2017**, *43*, 1371.
- 18 *Absorbable and Biodegradable Polymers*; S. W. Shalaby, K. J. L. Burg, Eds.; CRC Press: Boca Raton, FL, **2004**; pp 59.

- 19 F. Leonard, R. K. Kulkarni, G. Brandes, J. Nelson, J. J. Cameron, *J. Appl. Polym. Sci.* **1966**, *10*, 259.
- 20 C. Joch, *Cardiovasc. Surg.* **2003**, *11*, 23.
- 21 M. Radosevich, H. Goubran, T. Burnouf, *Vox Sang.* **1997**, *72*, 133.
- 22 M. Mehdizadeh, J. Yang, *J. Macromol. Biosci.* **2013**, *13*, 271.
- 23 N. A. Peppas, J. Z. Hilt, A. Khademhosseini, R. Langer, *Adv. Mater.* **2006**, *18*, 1345.
- 24 J. C. Wheat, J. S. Wolf, *Urol. Clin. North Am.* **2009**, *36*, 265.
- 25 D. Wallace, G. Cruise, W. Rhee, J. Schroeder, J. Prior, J. Ju, M. Maroney, J. Duronio, M. Ngo, T. Estridge, *J. Biomed. Mater. Res. A* **2001**, *58*, 545.
- 26 W. D. Spotnitz, S. Burks, *Transfusion* **2008**, *48*, 1502.
- 27 J. K. Tessmar, A. M. Göpferich, *J. Macromol. Biosci.* **2007**, *7*, 23.
- 28 R. A. Marklein, J. A. Burdick, *Soft Matter* **2010**, *6*, 136.
- 29 S. L. Fenn, R. A. Oldinski, *J. Biomed. Mater. Res. B: Appl. Biomater.* **2016**, *104*, 1229.
- 30 K. S. Lim, B. S. Schon, N. V. Mekhileri, G. C. Brown, C. M. Chia, S. Prabakar, G. J. Hooper, T. B. Woodfield, *ACS Biomater. Sci. Eng.* **2016**, *2*, 1752.
- 31 S. Lee, B. Lee, B. J. Kim, J. Park, M. Yoo, W. K. Bae, K. Char, C. J. Hawker, J. Bang, J. Cho, *J. Am. Chem. Soc.* **2009**, *131*, 2579.
- 32 P. Ferreira, J. Coelho, J. Almeida, M. Gil, *Biomedical Engineering-Frontiers and Challenges*; InTech: Vienna, Austria, **2011**.
- 33 G. Camci-Unal, D. Cuttica, N. Annabi, D. Demarchi, A. Khademhosseini, *Biomacromolecules* **2013**, *14*, 1085.
- 34 D. Loessner, C. Meinert, E. Kaemmerer, L. C. Martine, K. Yue, P. A. Levett, T. J. Klein, F. P. Melchels, A. Khademhosseini, D. W. Huttmacher, *Nat. Protoc.* **2016**, *11*, 727.
- 35 S. T. Koshy, T. C. Ferrante, S. A. Lewin, D. J. Mooney, *Biomaterials* **2014**, *35*, 2477.
- 36 J.-Y. Lai, Y.-T. Li, *Biomacromolecules* **2010**, *11*, 1387.
- 37 W. D. Spotnitz, S. Burks, *Transfusion* **2012**, *52*, 2243.
- 38 S. Féréol, R. Fodil, B. Labat, S. Galiacy, V. M. Laurent, B. Louis, D. Isabey, E. Planus, *Cytoskeleton* **2006**, *63*, 321.
- 39 J. Voigt, V. R. Driver, *Wound Repair Regen.* **2012**, *20*, 317.
- 40 X. Xu, A. K. Jha, D. A. Harrington, M. C. Farach-Carson, X. Jia, *Soft Mater.* **2012**, *8*, 3280.
- 41 M. Etscheid, N. Beer, J. Dodt, *Cell. Signal.* **2005**, *17*, 1486.
- 42 H. Zhu, N. Mitsunashi, A. Klein, L. W. Barsky, K. Weinberg, M. L. Barr, A. Demetriou, G. D. Wu, *Stem Cells* **2006**, *24*, 928.
- 43 X.-H. Qin, P. Gruber, M. Markovic, B. Plochberger, E. Klotzsch, J. Stampfl, A. Ovsianikov, R. Liska, *Polym. Chem.* **2014**, *5*, 6523.
- 44 S. K. Seidlits, Z. Z. Khaing, R. R. Petersen, J. D. Nickels, J. E. Vanscoy, J. B. Shear, C. E. Schmidt, *Biomaterials* **2010**, *31*, 3930.
- 45 J. B. Leach, K. A. Bivens, C. W. Patrick Jr, C. E. Schmidt, *Bio-technol. Bioeng.* **2003**, *82*, 578.
- 46 J. L. Ifkovits, E. Tous, M. Minakawa, M. Morita, J. D. Robb, K. J. Koomalsingh, J. H. Gorman, R. C. Gorman, J. A. Burdick, *Proc. Natl. Acad. Sci. U. S. A.* **2010**, *107*, 11507.
- 47 K. A. Smeds, M. W. Grinstaff, *J. Biomed. Mater. Res. A* **2001**, *54*, 115.
- 48 J. A. Burdick, C. Chung, X. Jia, M. A. Randolph, R. Langer, *Biomacromolecules* **2005**, *6*, 386.
- 49 L. Kima, R. L. Maucka, J. A. Burdick, *Biomaterials* **2011**, *32*, 8771.
- 50 M. H. Oudshoorn, R. Rissmann, J. A. Bouwstra, W. E. Hennink, *Polymer* **2007**, *48*, 1915.
- 51 B. H. Lee, H. Shirahama, N.-J. Cho, L. P. Tan, *RSC Adv.* **2015**, *5*, 106094.
- 52 H. Kim, W. H. Kong, K.-Y. Seong, D. K. Sung, H. Jeong, J. K. Kim, S. Y. Yang, S. K. Hahn, *Biomacromolecules* **2016**, *17*, 3694.
- 53 S. A. Bencherif, A. Srinivasan, F. Horkay, J. O. Hollinger, K. Matyjaszewski, N. R. Washburn, *Biomaterials* **2008**, *29*, 1739.
- 54 C. Li, G. Guan, R. Reif, Z. Huang, R. K. Wang, *J. R. Soc. Interface* **2012**, *9*, 831.
- 55 R. G. Wells, *Hepatology* **2008**, *47*, 1394.
- 56 M. Mehdizadeh, H. Weng, D. Gyawali, L. Tang, J. Yang, *Biomaterials* **2012**, *33*, 7972.
- 57 O. Jeon, J. E. Samorezov, E. Alsberg, *Acta Biomater.* **2014**, *10*, 47.
- 58 N. Lang, M. J. Pereira, Y. Lee, I. Friehs, N. V. Vasilyev, E. N. Feins, K. Ablasser, E. D. O'cearbhaill, C. Xu, A. Fabozzo, *Sci. Transl. Med.* **2014**, *6*, 218ra216.
- 59 M. Yao, A. Yaroslavsky, F. P. Henry, R. W. Redmond, I. E. Kochevar, *Lasers Surg. Med.* **2010**, *42*, 123.
- 60 D. Smart, *Adv. Drug Deliv. Rev.* **2005**, *57*, 1556.
- 61 C. Claaßen, M. H. Claaßen, V. Truffault, L. Sewald, G. N. E. Tovar, K. Borchers, A. Southan, *Biomacromolecules* **2017**, *19*, 42.
- 62 G. Yue, M. M. Trujillo-de Santiago, A. Alvarez, N. Tamayol, A. K. Annabi, *Biomaterials* **2015**, *73*, 254.
- 63 B. Johnson, D. Beebe, W. Crone, *Mater. Sci. Eng. C* **2004**, *24*, 575.
- 64 E. A. Kamoun, E.-R. S. Kenawy, X. Chen, *J. Adv. Res.* **2017**, *8*, 217.
- 65 H. Y. Yoon, H. Koo, K. Y. Choi, I. C. Kwon, K. Choi, J. H. Park, K. Kim, *Biomaterials* **2013**, *34*, 5273.